scientific reports

Check for updates

OPEN

A droplet-based microfluidic platform enables high-throughput combinatorial optimization of cyanobacterial cultivation

Jialan Cao[1]✉, David A. Russo[2], Ting Xie[1], G. Alexander Groß[1] & Julie A. Z. Zedler[3]✉

Cyanobacteria are fast-growing, genetically accessible, photoautotrophs. Therefore, they have attracted interest as sustainable production platforms. However, the lack of techniques to systematically optimize cultivation parameters in a high-throughput manner is holding back progress towards industrialization. To overcome this bottleneck, here we introduce a droplet-based microfluidic platform capable of one- (1D) and two-dimension (2D) screening of key parameters in cyanobacterial cultivation. We successfully grew three different unicellular, biotechnologically relevant, cyanobacteria: *Synechocystis* sp. PCC 6803, *Synechococcus elongatus* UTEX 2973 and *Synechococcus* sp. UTEX 3154. This was followed by a highly-resolved 1D screening of nitrate, phosphate, carbonate, and salt concentrations. The 1D screening results suggested that nitrate and/or phosphate may be limiting nutrients in standard cultivation media. Finally, we use 2D screening to determine the optimal N:P ratio of BG-11. Application of the improved medium composition in a high-density cultivation setup led to an increase in biomass yield of up to 15.7%. This study demonstrates that droplet-based microfluidics can decrease the volume required for cyanobacterial cultivation and screening up to a thousand times while significantly increasing the multiplexing capacity. Going forward, microfluidics have the potential to play a significant role in the industrial exploitation of cyanobacteria.

Cyanobacteria have attracted interest for sustainable biotechnology due to their fast photoautotrophic growth, minimal nutritional requirements, and metabolic capacity for heterologous product formation. Transfer of existing systems to an industrial scale is, however, still rare and yet to come of age. Despite this, the market for cyanobacterial products is rapidly growing and cyanobacteria already account for half of the European algae production[1]. The existing products, however, are largely limited to "Spirulina" (*Arthrospira* spp.) which can be grown in high pH and high salt conditions. To efficiently exploit cyanobacterial diversity, and increase their biotechnological relevance, several challenges need to be solved. One key aspect is strain-specific optimization of growth conditions. To achieve this, high-throughput screening methods that are suitable for studying cyanobacterial chassis are needed. Standard high throughput methods for heterotrophic systems, such as micro-well cultivation and live-cell monitoring systems, are often incompatible with cyanobacteria due to the requirement for controlled light exposure, extended cultivation periods and autofluorescence interference with optical measurements. In addition, increasing of throughput by reducing volume raises new challenges in terms of oxygen supply, evaporation control and homogeneity. Thus, it is of great importance to establish alternative, cost-efficient, technologies that allow high-throughput optimization of cyanobacterial cultivation. Here, microfluidics has the potential to tackle this challenge.

In microfluidics, liquids or gases are handled in technical channels with dimensions in the micrometer to lower millimeter range. The central idea is the miniaturization of large-scale technical laboratory processes to improve handling, material requirements and to enable process automation. The beginning of the twentieth century brought a tremendous boom in microfluidics research, leading to the development of numerous new microfluidic platforms like droplet microfluidics, paper analytical devices, organ-on-a-chip and open

[1]Department of Physical Chemistry and Microreaction Technology, Institute for Chemistry and Biotechnique, Ilmenau University of Technology, Weimarerstr. 32, 98693 Ilmenau, Germany. [2]Bioorganic Analytics, Institute for Inorganic and Analytical Chemistry, Friedrich Schiller University Jena, Lessingstr. 8, 07743 Jena, Germany. [3]Synthetic Biology of Photosynthetic Organisms, Matthias Schleiden Institute for Genetics, Bioinformatics and Molecular Botany, Friedrich Schiller University Jena, Dornburgerstr. 159, 07743 Jena, Germany. ✉email: jialan.cao@tu-ilmenau.de; julie.zedler@uni-jena.de

microfluidics[2]. Most of the above-mentioned platforms can be assigned to one of three main categories: continuous-flow, microarray, and droplet-based[3]. Continuous flow microfluidic systems are featured by the continuous manipulation and flow of a single-phase fluid through closed microchannels or conduits. Many reports are showing that continuous-flow systems have been successfully used in drug discovery applications[4]. However, this system is difficult to scale for high throughput screening. Furthermore, this format is limited by the fact that parabolic flow profiles are inherent. Due to this, analyte molecules are in close contact with the channel walls resulting in precipitation, fouling and contamination. In microarray microfluidic systems, the liquid phase is single-phase, but discrete volumes may be separated from the stream to undergo further processing. The advantages of this technique are ease of screening large number of different samples and easy coupling with current industry high-throughput screening technologies (e.g. microtiter plates). The major disadvantage of microarray systems is that robotics is required for high-throughput, and precise, handling of small volumes. In comparison to the methods previously described, droplet-based microfluidic systems present several advantages. First, they operate with discrete, physically separated, fluids in microchannels and exhibit the highest multiplex capability. Here, the sample or reagent phase is interrupted by a water-immiscible carrier phase, forcing it to split into discrete droplets. Since the droplets are separated from each other and the channel walls by the immiscible carrier phase, such droplets do not have the disadvantages that occur with continuous flows, such as fouling or contamination. The volume of droplets ranges from pL to nL, making the reaction volume roughly a thousand to a million times smaller than conventional cultivation conditions. Furthermore, various unit operations for droplet manipulation such as mixing, dilution, splitting, merging and incubation are readily available[5,6].

From an application point of view, droplet microfluidics is an established tool in chemical analytics and micro reaction technology and has played a pivotal role in the development of high-throughput analysis of biological systems. It was first recognized as a promising tool for biological applications more than two decades ago. Starting with micro capillary electrophoresis[7] and micro flow-through PCR[8,9], miniaturized fluidic techniques became of interest for fast and efficient bioanalytical procedures. The ability to miniaturize volumes and multiplex sample handling and analysis then also attracted interest in molecular biology as well as in microbiology. For cultivation, droplet-based microfluidics by micro segmented-flow was first introduced to separate soil microorganisms from complex soil microbial communities[10]. In small droplets, the principle of stochastic confinement applies. In other words, rare individuals and their released molecules can accumulate to high densities, thus, enabling single cell experiments[11–13]. The segmented-flow principle enables an easy screening of sample series with concentration gradients and allows the measurement of organismic responses to stress factors such as antibiotics, nanoparticles or heavy metals[14–16] with high resolution. In addition, this approach allows the screening of two and three-dimensional concentration spaces with a small amount of consumables in a single experimental run. Thus, opening the possibility of conveniently detecting combinatorial effects of, for example, toxins, pharmaceutical drugs and nutrients[17]. Furthermore, droplet-based microfluidics is in use for detection of antibiotic resistances and for the development of new antibiotics[18]. Besides bacteria, the micro segmented-flow technique has also proven to be suitable for eukaryotic microorganisms such as *Chlorella*[19] or even embryos of multicellular organisms[20] and for the characterization of the concentration-dependent response of complex unknown environmental bacterial communities on toxic substances[21,22]. As applied to cyanobacterial systems, microfluidics is an emerging technology with only a handful of applications. For instance, a microfluidic tool for harvesting cyanobacterial biomass was developed for *Synechocystis* sp. PCC 6803[23] (hereafter PCC 6803). In addition, microfluidic technology has been used for lactate productivity screening in a PCC 6803 CRISPRi library[24] as well as to screen for ethanol production[25].

Here, we established a droplet-based microfluidic setup that allows for high-throughput medium composition optimization for biotechnologically relevant cyanobacteria. We tested the compatibility of our system with three different cyanobacterial strains using biomass accumulation as the screening parameter. Our microfluidic setup allowed for continuous cultivation and analysis of the cells where individual medium parameters such as macronutrient content as well as salt and bicarbonate concentrations were varied in small steps allowing for highly parallel, high-throughput screening. In addition, we demonstrated that our platform is able to screen two parameters simultaneously to explore the two-dimensional effect space of combined variables. In conclusion, we demonstrate that microfluidics can be used to improve medium composition and cultivation conditions in a cost- and time-effective manner to unlock the exploitation of biotechnologically relevant cyanobacteria.

Materials and methods

Cyanobacterial strains and growth conditions. Three cyanobacterial wild-type strains were used: a non-motile, glucose-tolerant substrain of *Synechocystis* sp. PCC 6803 (originally obtained from Patrik Jones, Imperial College London), *Synechococcus elongatus* UTEX 2973 (originally obtained from Himadri Pakrasi, University of Washington) (hereafter UTEX 2973) and *Synechococcus* sp. UTEX 3154 (a spontaneous mutant of *Synechococcus* sp. PCC 11901[26] which does not require vitamin B_{12} for growth, obtained from the UTEX culture collection) (hereafter UTEX 3154). PCC 6803 and UTEX 2973 were grown in BG-11 medium[27] supplemented with 10 mM *N*-Tris(hydroxymethyl)methyl-2-aminoethanesulphonic acid (TES) buffer (pH 8.0) (BG-11 TES medium). Medium A[28] with D7 micronutrients[29] (AD7 medium) (pH 7.5) was used for cultivation of UTEX 3154. All cultures were maintained at 30 °C with 20–50 µmol photons m^{-2} s^{-1} white light [Lumilux cool white L 15 W/840 fluorescent lamps (Osram, Germany)] on BG-11 or AD7 medium plates supplemented with 1.5% bacto-agar. Liquid pre-cultures for inoculation of the microfluidic coils were grown in glass tubes bubbled with 3% CO_2-supplemented air at 30 °C with approximately 60 µmol photons m^{-2} s^{-1} white light for 3 to 4 days (mid-to-late exponential growth phase) (culture volume: 20 mL). These cultures were then counted and diluted with growth medium to obtain 10^7 cells mL^{-1} and used for droplet inoculation. The initial cell density of each droplet was 10 cells nL^{-1} with a total droplet volume of 500 nL.

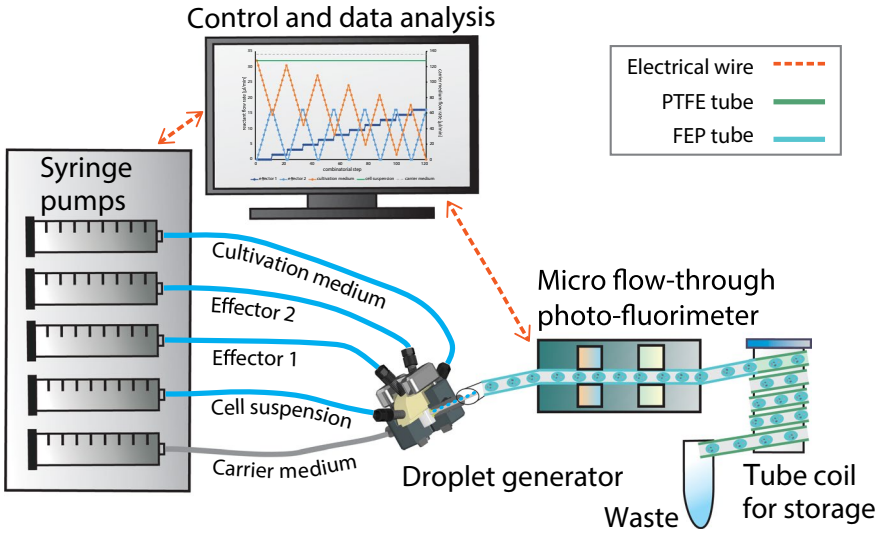

Figure 1. Experimental droplet-based microfluidic setup for 1D and 2D screening of cultivation parameters used in this study. The illustration on the left shows a 5-channel syringe pump and the droplet generator which generates the droplets. The individual aqueous cell medium droplets are separated by the immiscible carrier medium. Droplet size/volume, spacing and composition can be adjusted via the controlled flow rate program of the syringe pump. The generated droplets are measured by a combined photo-fluorimetric micro flow-through detector unit. The droplet sequences are then collected and incubated in PTFE tube coils in an internally illuminated incubator.

To test improved nitrogen:phosphorus (N:P) ratios based on 2D screening experiments, standard BG-11 medium and BG-11 medium with adjusted $NaNO_3$ and K_2HPO_4 concentrations were prepared. Liquid cultures were inoculated for PCC 6803 and UTEX 2973 in a high-density cultivation setup (HDC 6.10 starter kit CellDEG, Germany)[30] using 25 mL culture vessels with a culture volume of 10 mL. The cultures were supplemented through a membrane with CO_2 at a partial pressure of approximately 32 mbar (reference T = 20 °C) by a carbonate buffer (3 M $KHCO_3$ and 3 M K_2CO_3, ratio 4:1)[30]. The growth setup was placed on a Unimax 1010 orbital shaker (Heidolph Instruments, Germany) and incubated with shaking at 280 rpm at 30 °C with 50 µmol photons m^{-2} s^{-1} white light [Lumilux cool white L 15 W/840 fluorescent lamps (Osram, Germany)]. Main cultures for the growth experiment were inoculated in triplicates from a pre-culture grown in the same medium and conditions to a starting optical density (OD) at 750 nm of 0.3 and monitored for 7 days by measuring OD at 750 nm every 24 h using a GENESYS 10S UV–Vis Spectrophotometer (Thermo Scientific, Germany). For PCC 6803, the optimized BG-11 medium contained 0.4 mM K_2HPO_4 and 27 mM $NaNO_3$ and for UTEX 2973 0.45 mM K_2HPO_4 and 30 mM $NaNO_3$. All other elements of the medium were kept the same as in the standard BG-11 TES medium.

Microfluidic cultivation

Microfluidic arrangement. Details on the fluidic devices, the optical detection unit and the applied methods for realizing concentration-graded droplet sequences were reported earlier[15]. Here, a similar experimental setup (Fig. 1) was used for one- and two-dimensional screening of medium parameters. Briefly, the system is based on a syringe pump with six dosing units (Cetoni GmbH, Germany). The microfluidic droplets were generated by a self-developed droplet generator comprising of a 6-port manifold[31]. Droplets with varying compositions are generated by controlled dosing of effectors, culture medium and cell suspension into a flow of carrier liquid [perfluoromethyldecalin (PP9)] The droplet generator was connected via fluoroethylenepropylene (FEP) tubing (inner diameter 1.0 mm and outer diameter 1.6 mm) to the computer-operated syringe pump, utilizing syringes with volumes of 500 µL (effector solution and cell suspension), 1000 µL (culture medium) and 5000 µL (carrier liquid). Generated segments are transported at a constant flow rate of 200 µL min^{-1} through an optical detector unit for the simultaneous measurement of absorbance and fluorescence data of the droplets. Data were recorded directly through the visually transparent FEP tubing (Fig. 1). Absorbance was measured with four light emitting diodes (Agilent, United States) with peak wavelengths of 470, 505, 615 and 750 nm. Measurement of fluorescence was carried out with a laser diode with a peak wavelength of 405 nm (Changchun New Industries Optoelectronics, China) with a longpass filter (425 nm) (Laser Components, Germany) on the detection side. The emitted photons were recorded by a photomultiplier module (Hamamatsu, Japan). To store and incubate the generated droplet sequences, polytetrafluoroethylene (PTFE) tube coils (inner diameter 0.5 mm and outer diameter 1.6 mm) with a length of four meters for 1D and seven meters for 2D screening were used.

Experimental parameters. The syringe pump flow rates of the different fluids were controlled using a LabVIEW program (National Instruments, USA). To investigate the dose–response relationships for single substances (1D screening), a syringe pump control program with continuous change of the desired effector against

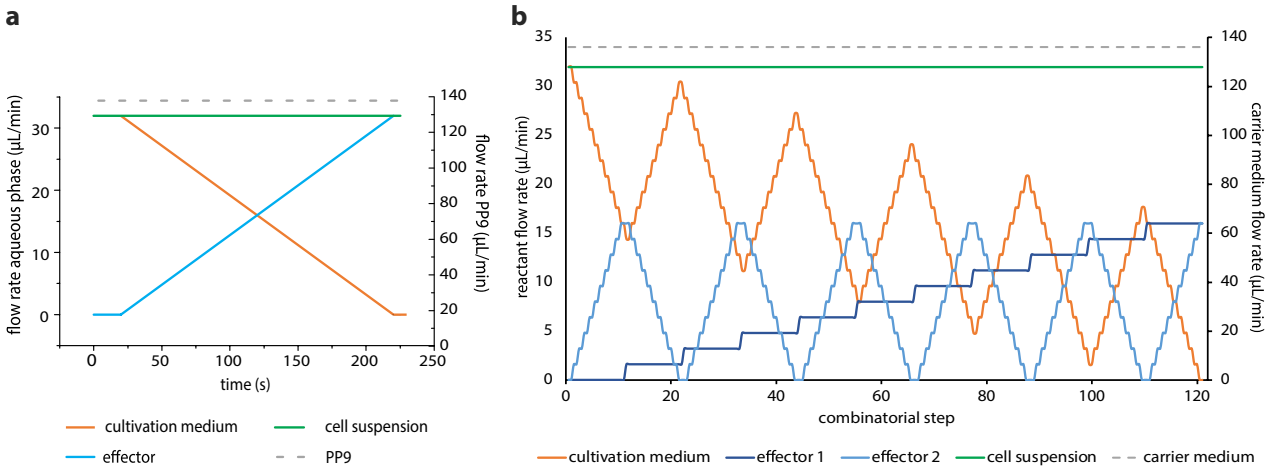

Figure 2. Syringe pump control program for the generation of 1D and 2D gradients. **(a)** Highly resolved dose response screening for single substances (1D screening). The base cultivation medium was continuously substituted over time by the effector-spiked medium and **(b)** two-dimensional concentration spaces in 11 combinatorial steps, resulting in 121 concentration combinations (2D screening).

a diluting medium was used (Fig. 2a). For two effectors (2D screening), a stepwise increase of the concentrations with a resolution of 10% was applied. Hence, for two effectors, 11 different concentration steps (0, 10, 20, 30, 40, 50, 60, 70, 80, 90, 100%) were combined resulting in 121 different combinations (Fig. 2b). The flow rates of the carrier liquid and the cell suspension were set to 136 µL min^{-1} and 32 µL min^{-1} respectively. The flow rates of the effector solutions and cultivation medium were varied within a total flow rate of 32 µL min^{-1}. Therefore, the overall flow rate of the segment generation process was kept constant at 200 µL min^{-1}. An initial cell density of 5000 cells per 500 nL segment (107 cells mL^{-1}) was applied. The generation of the highly resolved 1D and 2D screening sequences required approximately four and nine minutes. After droplet formation and initial photo-fluorimetric analysis (t = 0), the droplets were gathered in the subsequent collection tube coils for incubation. The tube coils were incubated for 7 days at 30 ± 2 °C, 3% CO2 and under 20 ± 5 µmol photons m^{-2} s^{-1} illumination. The different droplet sequences were analyzed daily by passing through the photo-fluorimetric detection unit to monitor cell density.

Effector screening concentration range. For effector screening, only the concentrations of our test variables were altered, while the remaining medium components were kept at the same concentrations. Stock solutions with two-fold concentrations for 1D screening and four-fold concentrations for 2D screening of the highest final concentration were prepared. These stocks were then used to generate highly resolved concentration gradients using the syringe pump control programs as shown in Figs. 1 and 2. In all experiments, PP9 (F2 Chemicals Ltd, Lancashire, UK) was used as an immiscible carrier liquid.

Data processing. The photo-fluorometric data were recorded with 250 Hz sampling rate. Droplet sequences were measured immediately after formation and after seven days of incubation in the coils (for the generation of growth curves, daily measurements were taken). The droplet data were analyzed offline using a custom LabVIEW program which elucidates droplet-specific data from the spectral sensor raw data: number, size, distance between two neighboring droplets as well as extinction and fluorescence measurements. Individual droplets were detected if the absorbance value exceeded the background and achieved a set threshold value. The droplet size correlates with the droplet passage time through the sensor and is determined by the time interval the absorbance exceeds a set threshold value. Due to the inhomogeneous cell distribution in the droplets, growth behavior was analyzed by calculating the integral of the absorbance and fluorescence signal with respect to the droplet size. The recorded autofluorescence intensity of the droplets $I(t)$ was normalized to the initial measurement intensity $I(t_0)$ using Eq. (1). Whereas the background was taken on the FEP-tube filled with carrier liquid. Data are given as normalized autofluorescence units (NFU).

$$NFU_t^{405/425} = \frac{I_t - I_{t_0}}{I_{t_0}} \quad (1)$$

Statistics and reproducibility. In total, the growth kinetic and 1D screening experiments were repeated three times and the 2D screening experiments two times. An example of a typical data distribution can be found in Supplementary Fig. 1 where each circle represents the intensity for an individual droplet. The droplets were then grouped into 32 concentration ranges from 0 to 100% of effector concentration (corresponding to a 3.1% concentration resolution). The mean and standard deviation were calculated for these 32 concentrations ranges and the resulting curve was plotted as a dose–response curve (Supplementary Fig. 1 blue triangles). For

the growth kinetic experiment, each data point represents the average and standard deviation of 50 ± 5 droplets across two independent coils. For 1D and 2D screening experiments, a total of 440 ± 21 and 814 ± 26 droplets, respectively, were generated per coil. These droplets were then distributed across the chemical gradients and approximately 10 (1D screening) and 8 (2D screening) droplets were analyzed per tested concentration. In sum, each data point represents the average and standard deviation of 20 ± 6 (1D screening) and 16 ± 6 (2D screening) droplets. This redundancy was applied in order to validate measurement reliability and to control for stochastic effects that can derive from small reaction volumes and cell numbers. Comparison of final biomass values in the high-density cultivation setup were done with an independent sample Student's t-test with a significance value of $\alpha = 0.05$.

Results and discussion

In this study we introduce a microfluidic method that allows us to rapidly screen one- and two-dimensional (1D and 2D) culture medium parameters to optimize the growth conditions of industrially relevant cyanobacteria. Our results show that our droplet-based microfluidic approach is well suited to screen culture media conditions in a fast and efficient way, with low material input and a reduced amount of incubator space. In addition, we observed that commonly used medium formulations are not optimized for maximum growth and small changes can result in significantly higher biomass outputs. This method should be widely applicable to a variety of freshwater and saltwater strains and has the potential to facilitate high-throughput strain optimization.

Both freshwater and marine unicellular cyanobacteria can be successfully cultivated in microdroplets. To test the applicability of microdroplet cultivation to cyanobacteria we chose three biotechnologically relevant species. PCC 6803 is a freshwater model cyanobacterium that has been extensively characterized and for which many molecular tools exist. UTEX 2973 is a freshwater fast-growing relative of *Synechococcus elongatus* PCC 7942. Due to their genetic proximity, an average nucleotide identity (ANI) > 99.8%[32], the tools developed for *Synechococcus elongatus* PCC 7942 are largely transferable to UTEX 2973. UTEX 2973 is of particular interest for biotechnological applications because of its fast growth phenotype with doubling times reported as fast as 1.5 h[33]. As a third strain, we chose a saltwater strain. A recently isolated strain, *Synechococcus* sp. PCC 11901 (hereafter PCC 11901), is genetically tractable and has clear biotechnological potential due to its reported doubling time of approximately 2 h and its ability to grow at high light intensities and a range of salinities. Under optimized conditions, PCC 11901 can accumulate up to 33 g of dry cell weight per liter. Curiously, it has an ANI of 96.76% when compared to the commonly used *Synechococcus* sp. PCC 7002 strain[26]. Therefore, it may be possible to utilize tools previously developed for *Synechococcus* sp. PCC 7002 in PCC 11901. However, this strain is a vitamin B_{12} auxotroph. Hence, we decided to use a closely related, spontaneous mutant of this strain, UTEX 3154, that can grow without an external supply of vitamin B_{12}.

First, we proceeded to test whether these three cyanobacterial strains could grow in the droplet-based microfluidic setup. For the initial screening, sensors detecting autofluorescence (excitation: 405 nm, emission: 425 nm) and optical density (OD) at 470, 505, 615 and 750 nm were tested over a period of 7 days. In our microfluidic setup, OD reflects the reduction of the intensity of transmitted light by use of a microflow-through photometer. OD typically correlates well with the final cell number. However it does not allow to distinguish between alive and dead cells. Growth can also be monitored by measuring the endogenous cellular autofluorescence with a micro flow-through fluorimeter. The fluorescence can be used to evaluate the approximate number of physiological active cells and, typically, is a more sensitive parameter than OD. The observed increase of the signals in all sensor channels clearly demonstrates cell growth (Supplementary Fig. 2, Supplementary Data Table S1). However, the highest intensities were observed in the OD_{470} (Fig. 3a) and the autofluorescence (Fig. 3b) channels. Therefore, in further experiments, we decided to use the autofluorescence channel to evaluate biomass accumulation. In some cases, biomass accumulation in the droplet storage coils was visible by the naked eye already after 4 days (Fig. 3c). The high cell density was confirmed by the observation of selected individual droplets by light microscopy (Fig. 3d). The typically reported doubling times for PCC 6803 are in the range of 10 to 12 h[34,35] and approximately 2 h for UTEX 2973[32] and UTEX 3154[26]. In line with this, our data show that PCC 6803 grows significantly slower than UTEX 2973 and UTEX 3154 (Fig. 3a,b). Between UTEX 2973 and UTEX 3154 we observed similar exponential growth rates and final biomass values despite the longer lag phase of UTEX 2973. Overall, the individual growth profiles fit with published literature[26,32,36] and show that microdroplet cultivation is suitable for unicellular freshwater and saltwater strains.

Microdroplet technology facilitates high-throughput, high-resolution dose response screening. Following the successful droplet-based cultivation of PCC 6803, UTEX 2973 and UTEX 3154, we proceeded to apply the methodology to investigate the response of the cyanobacteria to a variety of medium parameters. Therefore, we designed 1D screening experiments for media optimization. We used the standard growth medium for the respective strains (BG-11 for PCC 6803 and UTEX 2973, AD7 for UTEX 3154) and varied one parameter at a time by microfluidic means. The varied parameters included the nitrogen (N) source, phosphorus (P) source as well as medium salinity and sodium bicarbonate concentrations (Table 1). Furthermore, we proceeded to look at combinatorial effects using 2D screening where both the N and P concentrations were varied simultaneously. An overview of the concentration range of all tested effectors for 1D and 2D screening experiments is shown in Table 1. A summary of the optimum values for the medium parameters tested in the 1D screening is shown in Table 2.

We first started 1D testing of different concentrations of $NaNO_3$ ranging from 2 to 50 mM. The data show that the freshwater PCC 6803 and UTEX 2973 achieved maximum biomass values at approximately 10 and 20 mM $NaNO_3$, respectively (Fig. 4a, Supplementary Data Table S2). For the saltwater UTEX 3154, the maximum

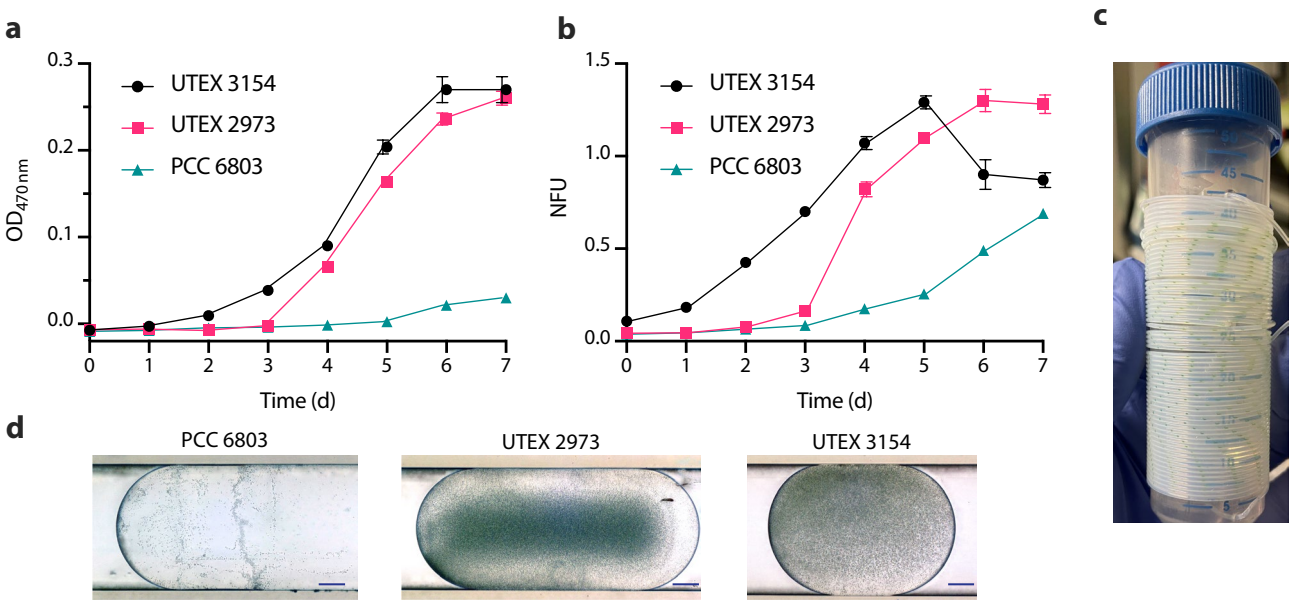

Figure 3. Growth of cyanobacteria in microdroplet setup. Growth kinetics of cyanobacterial strains (UTEX 3154, UTEX 2973 and PCC 6803) in the microfluidic coils measured with multi-channel photo-fluorimeter device showing **(a)** absorbance (optical density OD) at 470 nm and **(b)** normalized autofluorescence in the microfluidic setup over a 7 day period. Data points are averages of 50 ± 5 droplets. Error bars represent standard deviation. Normalized autofluorescence is shown as NFU. **(c)** Image of a microfluidic coil carrying UTEX 2973 droplets. **(d)** Light microscopy images of cyanobacteria PCC 6803, UTEX 2973 and UTEX 3154 in droplets after 4 days of growth (scale bar: 100 µm).

Medium component	1D screening range	2D screening range	BG-11 TES medium	AD7 medium
$NaNO_3$ (mM)	2–50	0–30	17.6	12
K_2HPO_4 (mM)	0.05–5	0–0.5	0.175	–
KH_2PO_4 (mM)	0.05–5	0–0.5	–	0.37
$NaHCO_3$ (mM)	0–100	–	–	–
NaCl (mM)	0–1300	–	–	308

Table 1. Range of concentrations for 1D and 2D screening experiments of selected medium components used in this study. Reference values of concentrations in standard BG-11 TES and AD7 medium are given.

Medium component	PCC 6803	UTEX 2973	UTEX 3154
$NaNO_3$ (mM)	10	20	30
K_2HPO_4 (mM)	2.5–3.5	0–0.5	–
KH_2PO_4 (mM)	–	–	0.75
$NaHCO_3$ (mM)	50	NS	NS
NaCl (mM)	100–650	0–300	0–1100

Table 2. Summary of the concentration ranges where the highest growth was observed in the 1D screening.

biomass value was achieved at approximately 30 mM $NaNO_3$ (Fig. 4a). The typical concentration of $NaNO_3$ present in the freshwater cyanobacterial growth medium BG-11 is 17.6 mM. Comparing this value with the limiting $NaNO_3$ concentrations for PCC 6803 and UTEX 2973 (10 and 20 mM, respectively), we can conclude that N is not typically the limiting nutrient in BG-11 medium. Accordingly, an earlier study showed that during batch cultivation of PCC 6803 in BG-11 medium one of the major medium limitations may be sulfate ions[37]. Regarding the saltwater medium AD7, the concentration of $NaNO_3$ is 12 mM. Considering that the biomass accumulation of UTEX 3154 only peaked at around 30 mM $NaNO_3$, our data suggest that N may be a limiting nutrient in AD7. This is supported by the original PCC 11901 strain publication where the authors determined the ideal $NaNO_3$ concentration to be between 24 and 48 mM[26]. Overall, these data show that, given enough N, all three cyanobacteria are rapidly limited by other nutrients. Therefore, we proceeded to apply our microfluidic

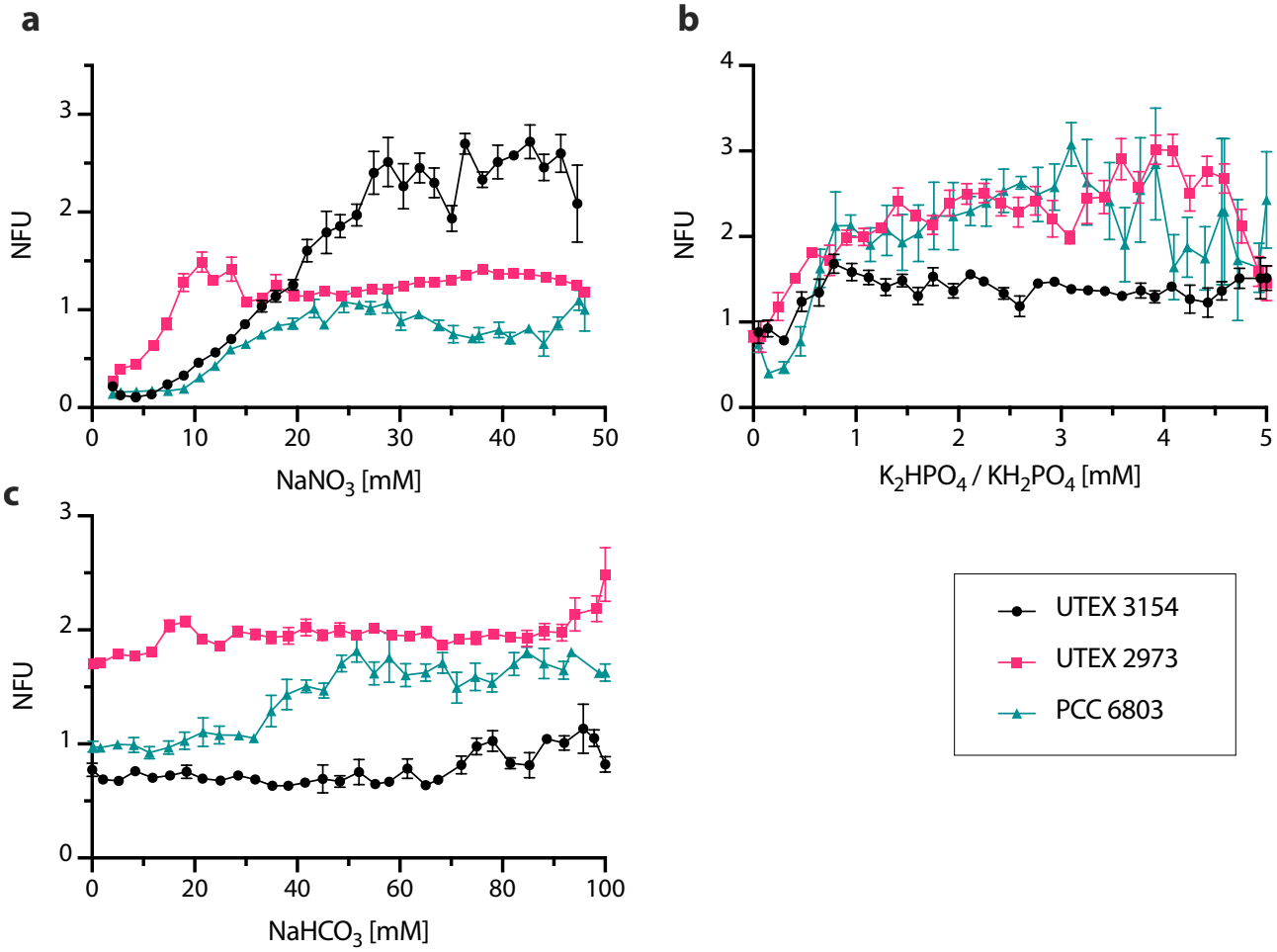

Figure 4. Highly resolved dose–response screenings of key macronutrients in UTEX 3154, UTEX 2973 and PCC 6803. **(a)** Normalized autofluorescence after 7 days in response to varying concentrations of $NaNO_3$. **(b)** Normalized autofluorescence after 7 days in response to varying concentrations of K_2HPO_4 (UTEX 2973, PCC 6803) or KH_2PO_4 (UTEX 3154). **(c)** Normalized autofluorescence after 7 days in response to varying concentrations of bicarbonate ($NaHCO_3$). Data points are averages of 10 ± 3 droplets. Error bars represent standard deviation. Normalized autofluorescence is shown as NFU.

approach to test the effect of varying concentrations of phosphate (K_2HPO_4 for UTEX 2973 and PCC 6803 and KH_2PO_4 for UTEX 3154) up to a maximum concentration of 5 mM. The data show that the maximum biomass values were achieved between 2.5 and 3.5 mM phosphate for PCC 6803 and UTEX 2973 and 0.75 mM phosphate for UTEX 3154 (Fig. 4b, Supplementary Data Table S3). Looking at the formulations of the base medium, phosphate is present at a concentration of 0.175 mM K_2HPO_4 in BG-11 and 0.37 mM KH_2PO_4 in AD7. Therefore, our microfluidic growth data suggest that both media are P deficient. This is particularly the case for BG-11 which has a K_2HPO_4 concentration 5 to 6 times lower than the levels at which we observed the highest biomass accumulation. It has been suggested that media designed for the growth of algae and cyanobacteria are often P limited due to a lack of compatibility with the Redfield ratio[38]. This ratio describes the amount of carbon (C), N and P typically present in both phytoplankton biomass and in dissolved nutrient pools and has been determined to be 106 C:16 N: 1 P. Based on the media formulation used in the study, AD7 presents a N:P ratio of 32:1 and BG-11 100:1. Thus, supporting our previous hypothesis that both media, and BG-11 in particular, may be P limited.

The autotrophic growth of cyanobacteria requires a source of inorganic C which is typically provided as CO_2. CO_2 can be supplied by air (0.04% CO_2), CO_2 enriched air (typically 1–5%) or in the form of bicarbonate salts. Installing a gas supply to cyanobacterial cultures can be costly and presents a logistical challenge for parallel experimentation. Therefore, sodium bicarbonate is a popular low-cost inorganic C source for cyanobacterial medium. Here, we tested the addition of $NaHCO_3$ to BG-11 and AD7 in the range of 0 to 100 mM (Fig. 4c, Supplementary Data Table S4). The addition of bicarbonate improved the growth of PCC 6803 from 35 mM and achieved a maximum biomass accumulation at approximately 50 mM. For UTEX 2973 and UTEX 3154 there was no significant difference in biomass accumulation in the tested range. In our previous experiments we have shown that BG-11 is P limited (Fig. 4b). This could explain the lack of response of UTEX 2973 to the varying bicarbonate concentrations. In regard to UTEX 3154, a previous study in *Synechococcus* sp. PCC 7002 showed that significant biomass accumulation was only visible with bicarbonate concentrations higher than 500 mM[39]. This suggests that the range tested here may not comprise the ideal bicarbonate values for this cyanobacterium.

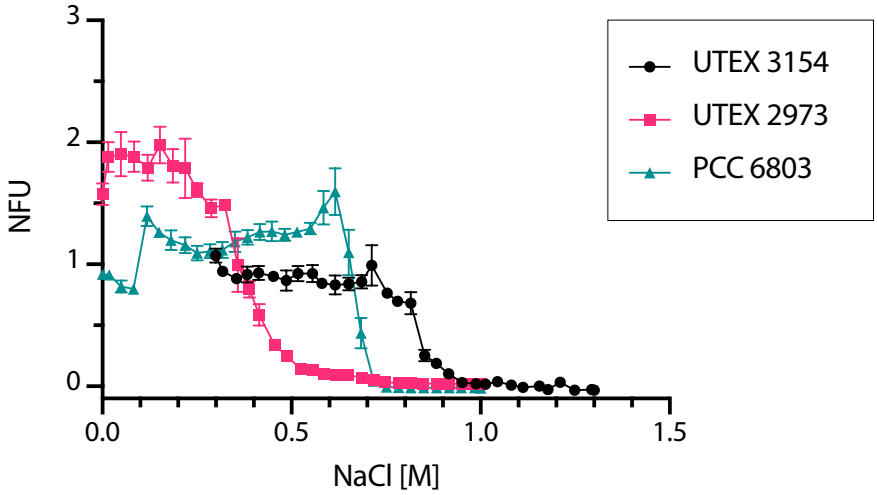

Figure 5. 1D screening of NaCl tolerance in cyanobacteria. Normalized autofluorescence after 7 days in response to varying concentrations of NaCl shown for three different cyanobacterial strains, UTEX 3154, UTEX 2973 and PCC 6803. Data points are averages of 10 ± 3 droplets. Error bars represent standard deviation. Normalized autofluorescence is shown as NFU.

However, *Synechococcus* sp. PCC 7002 and UTEX 3154 present significant genetic differences therefore it is difficult to make definite conclusions. Finally, another factor could be light limitation. In our experiments we used 20 ± 5 µmol photons m^{-2} s^{-1}, while the maximum growth rates of UTEX 2973 were reported at 1500 µmol photons m^{-2} s^{-1}, 42 °C and 5% CO_2[33]. However, this is not directly comparable as the light path in our microfluidic setup is 1.0 mm as opposed to the 27 mm used to determine the maximum growth rates of UTEX 2973 in the literature. Further tests would be needed to establish a robust comparison.

Salinity of the growth medium is a critical factor as high salinities can induce a variety of stresses and consequently pose a challenge to cell survival[40]. In addition, future large-scale cultivation of cyanobacteria should be done in seawater due to the limited freshwater resources present on Earth. Therefore, there has been an increased interest in prospecting for and developing salt-tolerant cyanobacterial chassis. Here, we used our microfluidic platform to determine the salt tolerance of PCC 6803, UTEX 2973 and UTEX 3154 (Fig. 5, Supplementary Data Table S5). As expected, the two freshwater strains exhibit lower salt tolerances than UTEX 3154. UTEX 2973 exhibits the lowest salt tolerance with a decline in biomass accumulation starting at 0.3 M NaCl. PCC 6803 maintains similar levels of biomass accumulation until 0.65 M with a sharp decline observed thereafter. Total inhibition was observed of both PCC 6803 and UTEX 2973 at 0.7 M NaCl. UTEX 3154 accumulates similar biomass levels until approximately 0.8 M, whereafter a sharp decline is also observed. It is worth noting here that the base AD7 used in this study contains 308 mM NaCl and 8 mM KCl therefore the data show that UTEX 3154 can tolerate salt concentrations up to 1.1 M NaCl. These values are in accordance with the published literature on salt tolerance in cyanobacteria[41]. Our data show that this microfluidic setup can be used for high-resolution screening for optimum salinity cultivation conditions of single-celled cyanobacteria and could serve as an effective high-throughput method to screen for strains with increased salt tolerance in future studies.

Simultaneous screening of phosphorus and nitrogen is essential for medium optimization. The above results demonstrate that our microfluidic platform can rapidly generate droplet screening sequences with a wide range of varying parameters (i.e. 1D screening). However, it is often of interest to screen a combination of parameters. Therefore, we took advantage of the capabilities of the droplet-based technique to simultaneously vary two independent parameters (2D screening). The results of a 2D medium optimization experiment are 2D response diagrams where we can easily estimate the effect of the two variables on one readout parameter (e.g. biomass accumulation). For the 2D proof of concept experiment we decided to screen N ($NaNO_3$) and P (K_2HPO_4 or KH_2PO_4) sources in conjunction (Fig. 6, Supplementary Data Table S6, S7, S8). These two parameters were chosen because the N:P ratio is one of the key parameters that influences algal growth and rapidly optimizing N and P concentrations is fundamental for cost-efficient scale-up of microalgal cultures[42]. Our data show that final biomass values in PCC 6803 and UTEX 2973 peaked at the maximum N values tested (0.45 mM K_2HPO_4/30 mM $NaNO_3$ for PCC 6803 and 0.4 mM K_2HPO_4/30 mM $NaNO_3$ for UTEX 2973) (Fig. 6a,b). Interestingly, an increase in N at low P values or an increase of P at low N values was not sufficient to obtain high biomass values. Only when both parameters were increased simultaneously was a significant increase in final biomass values observed. This contrasts with the conclusions from the 1D screening data where P seemed to be limiting the culture. This suggests that it is more efficient to find a good balance between N and P instead of just increasing one parameter. Therefore, 2D screening is fundamental to understanding nutrient dynamics in cyanobacterial cultures. Regarding the N:P ratio, both strains achieved their maximum biomass values at a ratio of approximately 100:1. This is the same ratio as BG-11 which suggests that the classic cyanobacterial medium has a good N:P ratio but would benefit from higher concentrations of both N and P. For UTEX

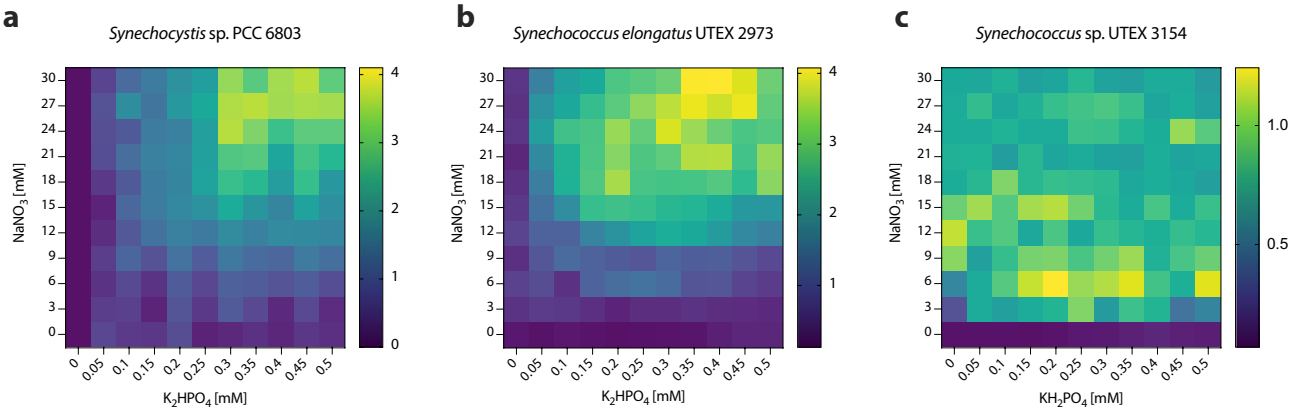

Figure 6. 2D screening of nitrogen and phosphorus source in cyanobacterial cultivation using standard growth media. **(a)** PCC6803 normalized autofluorescence after 7 days in response to varying concentrations of $NaNO_3$ and K_2HPO_4 in BG-11 medium. **(b)** UTEX 2973 normalized autofluorescence after 7 days in response to varying concentrations of $NaNO_3$ and K_2HPO_4 in BG-11 medium. **(c)** UTEX 3154 normalized autofluorescence after 7 days in response to varying concentrations of $NaNO_3$ and KH_2PO_4 in AD7 medium. Data points are averages of approximately 5 ± 3 droplets.

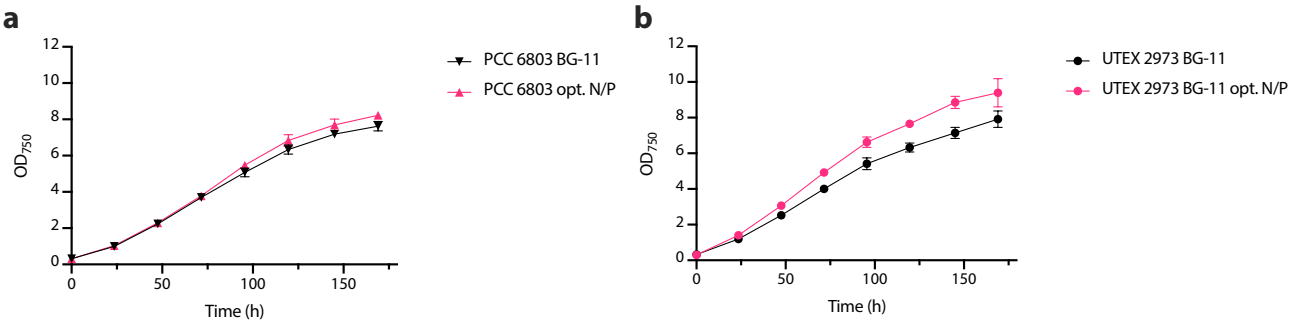

Figure 7. High-density cultivation in BG-11 medium containing N:P ratios optimized through 2D microfluidic screening. Growth of **(a)** PCC 6803 and **(b)** UTEX 2973 in standard vs. optimized N/P ratio observed by measuring optical density (OD) at 750 nm. n = 3 and error bars represent standard deviation.

3154 no clear trend was observed within the tested N:P range (Fig. 6c). Together with the 1D screening data, this suggests that N may be the limiting nutrient in the AD7. However, the possibility that a nutrient other than N or P limits the culture remains open.

Improved N:P ratios significantly increase biomass accumulation in high density cultivation. To assess whether the optimal N:P concentrations suggested by the microfluidic 2D experiments can be translated to a larger scale cultivation setup, we carried out growth assays in a laboratory setting. To this end, PCC 6803 and UTEX 2973 were grown in 25 mL high-density cultivators where gaseous CO_2 is supplied via integrated semi-permeable membranes. With this setup, growth was compared in standard BG-11 medium (0.175 mM K_2HPO_4, 17.6 mM $NaNO_3$) and BG-11 with the optimized N:P concentrations obtained from the 2D N:P microfluidic screening experiment. More specifically, 0.45 mM K_2HPO_4 with 30 mM $NaNO_3$ for PCC 6803 and 0.4 mM K_2HPO_4 with 30 mM $NaNO_3$ for UTEX 2973. For both PCC 6803 and UTEX 2973 significant increases ($p < 0.05$) of final biomass values of 7.4% (Fig. 7a) and 15.7% (Fig. 7b), respectively, could be observed. Overall, this confirmed that the findings from the microfluidic experiments are transferable to biotechnologically relevant high-density cultivation setups.

Droplet microfluidics significantly increases the multiplexing capacity of cyanobacterial cultivation. The cyanobacterial cultivation method that offers the highest multiplex capability is currently the microtiter plate (MTP). Assuming a 96-well MTP with 200 µL in each well, and that each microdroplet is the functional equivalent of a well on an MTP, we can establish a comparison between a MTP and the microfluidic approach established in this work. For example, for a 1% concentration resolution of a single substance (1D screening), 100 concentration steps are required. If 10 droplets are screened per concentration step, this is a total of 1000 droplets. With a volume of 0.2 µL/droplet, a total of 200 µL of medium is required in the microfluidic reactor. On the other hand, for the same experiment in an MTP, this would require 200 mL of medium across 10 MTPs. For the same 1% resolution in the case of a binary mixture (2D screening), 10,000 concentration steps are required. Therefore, a total of 2 mL of medium is required in the microfluidic reactor. To screen the same

amount of effector combinations in a MTP, 2L of medium across 100 MTPs would be required. The entire microfluidic preparation process, including cell counting and dilution, medium and effector preparation, sequence generation and measurement requires approximately 4 h. For 1D screening, the preparation of 10 MTPs with 100 concentration steps could feasibly be achieved in 4 h, albeit with a much higher risk of error. However, when moving to 2D screening, the preparation and cultivation of 100 MTPs becomes unfeasible. With droplet microfluidics, the move from 1 to 2D screening requires very little extra preparation time and the experimental footprint remains the same.

Conclusions

To achieve cost-effective scale-up of cyanobacteria it is crucial to screen for the ideal cultivation conditions. In particular, medium optimization can significantly increase biomass and product yields. However, the cost and time investment required to test different levels of key nutrients, and the possible interactions amongst them, is prohibitive with standard cultivation methods. Recently, miniaturized multiplex screening (e.g. microfluidics) has been suggested as a route to tackle the large parameter field of medium optimization. In this study we used a droplet-based microfluidic technique to improve the cultivation of three different biotechnologically relevant cyanobacterial strains. Our proof of concept demonstrated that the strains could be successfully cultivated with a medium requirement one thousand times lower than MTPs. Furthermore, growth data could be collected online with non-invasive, in-situ, measurements. The 1D screening data confirmed that our microfluidic platform is well-suited for the investigation of cyanobacterial response towards single nutrients. In addition, the 2D screening allowed us to explore the two-dimensional space of nutrient interactions with only a small increase in the time and reagents required. In conclusion, this study shows that microfluidics can play a valuable role in improving the cost-effectiveness of cyanobacterial cultivation. We also expect that this microfluidic approach can be generalized to other applications such as expression level optimization of engineered cyanobacteria and bioprospecting.

Data availability

All cyanobacterial strains used in this study are available from the Pasteur Culture Collection, Paris (France) or the UTEX Culture Collection of Algae, University of Texas, Austin (USA). The raw data of all experiments are provided in the Supplementary Data files.

Received: 9 July 2022; Accepted: 5 September 2022
Published online: 15 September 2022

References

1. Araújo, R. *et al.* Current status of the algae production industry in Europe: An emerging sector of the blue bioeconomy. *Front. Mar. Sci.* **7**, 626389 (2021).
2. Convery, N. & Gadegaard, N. 30 years of microfluidics. *Micro Nano Eng.* **2**, 76–91 (2019).
3. Dressler, O. J., Maceiczyk, R. M., Chang, S.-I. & de Mello, A. J. Droplet-based microfluidics: Enabling impact on drug discovery. *SLAS Discov.* **19**, 483–496 (2014).
4. Watts, P. & Haswell, S. J. Continuous flow reactors for drug discovery. *Drug Discov. Today* **8**, 586–593 (2003).
5. Shang, L., Cheng, Y. & Zhao, Y. Emerging droplet microfluidics. *Chem. Rev.* **117**, 7964–8040 (2017).
6. Kielpinski, M. *et al.* Microfluidic chamber design for controlled droplet expansion and coalescence. *Micromachines* **11**, 394 (2020).
7. Harrison, D. J. *et al.* Micromachining a miniaturized capillary electrophoresis-based chemical analysis system on a chip. *Science* **261**, 895–897 (1993).
8. Kopp, M. U., de Mello, A. J. & Manz, A. Chemical amplification: Continuous-flow PCR on a chip. *Science* **280**, 1046–1048 (1998).
9. Schneegaß, I. & Köhler, J. M. Flow-through polymerase chain reactions in chip thermocyclers. *Rev. Mol. Biotechnol.* **82**, 101–121 (2001).
10. Köhler, J. M. *et al.* Digital reaction technology by micro segmented flow—Components, concepts and applications. *Chem. Eng. J.* **101**, 201–216 (2004).
11. Debs, B. E., Utharala, R., Balyasnikova, I. V., Griffiths, A. D. & Merten, C. A. Functional single-cell hybridoma screening using droplet-based microfluidics. *Proc. Natl Acad. Sci. USA* **109**, 11570–11575 (2012).
12. Boedicker, J. Q., Li, L., Kline, T. R. & Ismagilov, R. F. Detecting bacteria and determining their susceptibility to antibiotics by stochastic confinement in nanoliter droplets using plug-based microfluidics. *Lab Chip* **8**, 1265–1272 (2008).
13. Täuber, S., Golze, C., Ho, P., von Lieres, E. & Grünberger, A. dMSCC: a microfluidic platform for microbial single-cell cultivation of *Corynebacterium glutamicum* under dynamic environmental medium conditions. *Lab Chip* **20**, 4442–4455 (2020).
14. Funfak, A., Cao, J., Knauer, A., Martin, K. & Köhler, J. M. Synergistic effects of metal nanoparticles and a phenolic uncoupler using microdroplet-based two-dimensional approach. *J. Environ. Monit.* **13**, 410–415 (2011).
15. Cao, J. *et al.* Uncovering toxicological complexity by multi-dimensional screenings in microsegmented flow: Modulation of antibiotic interference by nanoparticles. *Lab Chip* **12**, 474–484 (2012).
16. Kaminski, T. S., Scheler, O. & Garstecki, P. Droplet microfluidics for microbiology: techniques, applications and challenges. *Lab Chip* **16**, 2168–2187 (2016).
17. Cao, J., Goldhan, J., Martin, K. & Köhler, J. M. Investigation of mixture toxicity of widely used drugs caffeine and ampicillin in the presence of an ACE inhibitor on bacterial growth using droplet-based microfluidic technique. *Green Process Synth.* **2**, 591–601 (2013).
18. Mahler, L. *et al.* Highly parallelized droplet cultivation and prioritization of antibiotic producers from natural microbial communities. *Elife* **10**, e64774 (2021).
19. Kürsten, D., Cao, J., Funfak, A., Müller, P. & Köhler, J. M. Cultivation of *Chlorella vulgaris* in microfluid segments and microtoxicological determination of their sensitivity against $CuCl_2$ in the nanoliter range. *Eng. Life Sci.* **11**, 580–587 (2011).
20. Funfak, A., Brösing, A., Brand, M. & Köhler, J. M. Micro fluid segment technique for screening and development studies on *Danio rerio* embryos. *Lab Chip* **7**, 1132–1138 (2007).
21. Cao, J., Chande, C., Kalensee, F., Schüler, T. & Köhler, M. Microfluidically supported characterization of responses of *Rhodococcus erythropolis* strains isolated from different soils on Cu-, Ni-, and Co-stress. *Braz. J. Microbiol.* **52**, 1405–1415 (2021).
22. Kürsten, D. *et al.* Identification of response classes from heavy metal-tolerant soil microbial communities by highly resolved concentration-dependent screenings in a microfluidic system. *Methods Ecol. Evol.* **6**, 600–609 (2015).
23. Wang, L. & Dandy, D. S. A microfluidic concentrator for cyanobacteria harvesting. *Algal Res.* **26**, 481–489 (2017).

24. Yao, L. *et al.* Pooled CRISPRi screening of the cyanobacterium *Synechocystis* sp PCC 6803 for enhanced industrial phenotypes. *Nat. Commun.* **11**, 1666 (2020).
25. Abalde-Cela, S. *et al.* High-throughput detection of ethanol-producing cyanobacteria in a microdroplet platform. *J. R. Soc. Interface* **12**, 20150216 (2015).
26. Włodarczyk, A., Selão, T. T., Norling, B. & Nixon, P. J. Newly discovered *Synechococcus* sp. PCC 11901 is a robust cyanobacterial strain for high biomass production. *Commun. Biol.* **3**, 1–14 (2020).
27. Stanier, R. Y., Kunisawa, R., Mandel, M. & Cohen-Bazire, G. Purification and properties of unicellular blue-green algae (order Chroococcales). *Bacteriol. Rev.* **35**, 171–205 (1971).
28. Stevens, S. E., Patterson, C. O. P. & Myers, J. The production of hydrogen peroxide by blue-green algae: A survey. *J. Phycol.* **9**, 427–430 (1973).
29. Arnon, D. I., McSwain, B. D., Tsujimoto, H. Y. & Wada, K. Photochemical activity and components of membrane preparations from blue-green algae. I. Coexistence of two photosystems in relation to chlorophyll *a* and removal of phycocyanin. *Biochim. Biophys. Acta Bioenerg.* **357**, 231–245 (1974).
30. Bähr, L., Wüstenberg, A. & Ehwald, R. Two-tier vessel for photoautotrophic high-density cultures. *J. Appl. Phycol.* **28**, 783–793 (2016).
31. Cao, J. *et al.* Droplet-based screening for the investigation of microbial nonlinear dose-response characteristics system, background and examples. *Micromachines* **11**, 577 (2020).
32. Yu, J. *et al. Synechococcus elongatus* UTEX 2973, a fast growing cyanobacterial chassis for biosynthesis using light and CO_2. *Sci. Rep.* **5**, 8132 (2015).
33. Ungerer, J., Lin, P.-C., Chen, H.-Y. & Pakrasi, H. B. Adjustments to photosystem stoichiometry and electron transfer proteins are key to the remarkably fast growth of the cyanobacterium *Synechococcus elongatus* UTEX 2973. *MBio* **9**, e02327-e2417 (2018).
34. Vermass, W. F. J., Rutherford, A. W. & Hansson, Ö. Site-directed mutagenesis in photosystem II of the cyanobacterium *Synechocystis* sp. PCC 6803: Donor D is a tyrosine residue in the D2 protein. *Proc. Natl Acad. Sci. USA* **85**, 8477–8481 (1988).
35. Howitt, C. A., Udall, P. K. & Vermaas, W. F. J. Type 2 NADH dehydrogenases in the cyanobacterium *Synechocystis* sp. strain PCC 6803 are involved in regulation rather than respiration. *J. Bacteriol.* **181**, 3994–4003 (1999).
36. Eungrasamee, K., Miao, R., Incharoensakdi, A., Lindblad, P. & Jantaro, S. Improved lipid production via fatty acid biosynthesis and free fatty acid recycling in engineered *Synechocystis* sp. PCC 6803. *Biotechnol. Biofuels* **12**, 8 (2019).
37. van Alphen, P., AbediniNajafabadi, H., Branco dos Santos, F. & HellingwerfKlaas, J. Increasing the photoautotrophic growth rate of *Synechocystis* sp. PCC 6803 by identifying the limitations of its cultivation. *Biotechnol. J.* **13**, 1700764 (2018).
38. Kim, H. W., Vannela, R., Zhou, C. & Rittmann, B. E. Nutrient acquisition and limitation for the photoautotrophic growth of *Synechocystis* sp. PCC6803 as a renewable biomass source. *Biotechnol. Bioeng.* **108**, 277–285 (2011).
39. De Farias Silva, C. E., Gris, B., Sforza, E., La Rocca, N. & Bertucco, A. Effects of sodium bicarbonate on biomass and carbohydrate production in *Synechococcus* PCC 7002. *Chem. Eng. Trans.* **49**, 241–246 (2016).
40. Pade, N. & Hagemann, M. Salt acclimation of cyanobacteria and their application in biotechnology. *Life* **5**, 25–49 (2015).
41. Cui, J., Sun, T., Chen, L. & Zhang, W. Engineering salt tolerance of photosynthetic cyanobacteria for seawater utilization. *Biotechnol. Adv.* **43**, 107578 (2020).
42. Slade, R. & Bauen, A. Micro-algae cultivation for biofuels: Cost, energy balance, environmental impacts and future prospects. *Biomass Bioenerg.* **53**, 29–38 (2013).

Acknowledgements

We thank Prof. Michael Köhler for the fruitful discussion. We thank Frances Möller and Steffen Schneider for lab assistance. JC gratefully acknowledges financial support from the project "Screen | in drop lines" (2016FE9016) by Thüringer Aufbaubank and a habilitation scholarship from the TU Ilmenau, DAR was supported by the Alexander von Humboldt Foundation and by the IMPULSE^{project} (IP-2020-03, Friedrich Schiller University Jena). This work was funded by the Deutsche Forschungsgemeinschaft (DFG, German Research Foundation) under Germany's Excellence Strategy—EXC 2051—Project-ID 390713860 (JAZZ) and the by the Deutsche Forschungsgemeinschaft (DFG, German Research Foundation)—CRC 1127/2—239748522 (JAZZ).

Author contributions

Conceptualization and study design: J.C., D.A.R. and J.A.Z.Z. Experimental work and data analysis: J.C., D.A.R., T.X. and J.A.Z.Z. Microfluidic device and system development: G.A.G., J.C. Writing—original draft: J.C., D.A.R. and J.A.Z.Z. Writing—review & editing: J.C., D.A.R., G.A.G. and J.A.Z.Z. Funding acquisition and project administration: J.C., D.A.R., G.A.G. and J.A.Z.Z. All authors have read and approved the final manuscript.

Funding

Open Access funding enabled and organized by Projekt DEAL.

Competing interests

The authors declare no competing interests.

Additional information

Supplementary Information The online version contains supplementary material available at https://doi.org/10.1038/s41598-022-19773-6.

Correspondence and requests for materials should be addressed to J.C. or J.A.Z.Z.